Military Technical College
Kobry Elkobbah,
Cairo, Egypt
May 27-29,2008

4th International Conference on
Mathematics and Engineering
Physics (ICMEP-4)

WP-2

DEVELOPMENTS IN ELASTOMERIC OPTICS AT ATENEO DE MANILA UNIVERSITY

Raphael A. Guerrero, Ph.D.
Dept. of Physics, Ateneo de Manila University
Loyola Heights, Quezon City, Philippines
Tel: 63-2-426-6001 loc 5692, Fax: 63-2-426-1043
Email: rguerrero@admu.edu.ph

I. INTRODUCTION

Elastomeric materials allow the fabrication of controllable optical elements easily tailored for a specific application at a minimum of cost. At the Photonics Laboratory of Ateneo de Manila University, our group has made progress in developing deformable silicone-based devices for various optical systems. In this seminar, a survey of current technologies involving elastomeric optics, as well as plans for future work, will be presented. The discussion is divided into four major parts: multiplexed holographic data storage with an elastic phase mask, dynamic diffraction grating replicas with enhanced efficiency, fluorescent dye-doped elastomers, and basic experiments for grade school students employing silicone optics.

II. MULTIPLEXED HOLOGRAPHIC STORAGE WITH ELASTOMER PHASE MASKS

Massive data capacities and instantaneous access to information are the most attractive features of volume holographic storage systems. Several multiplexing methods involving various optical parameters are available for realizing the storage potential of volume holograms. In this section, a novel technique for phase-multiplexed holographic storage is reported [1]. Animation using volume holography is a fairly uncharted field of research and the optical storage method described here lends itself easily to video applications. Holographic video, in its most basic form, involves the sequential reconstruction of stored images, optimally at a rate of 25 frames per second (fps). A relatively simple set-up involves recording each video frame with random phase information and reconstructing the images in real time by altering the phase. Only one reference beam is used and the holographic medium remains stationary throughout recording and readout. Experiments in this current work present, to the best of the author's knowledge, the first demonstration of multiplexed holographic storage employing a silicone phase mask.

Silicone is an ideal material for phase masks due to its transparency and the relative ease with which phase information can be tailored for a specific use. The low cost of this elastomer also makes silicone phase masks a viable alternative to phase modulation using expensive SLM technology. Images are stored at different phase addresses determined by the displacement of the elastomer from an unstretched configuration. By alternately stretching and relaxing the phase mask, images are reconstructed sequentially in real time, leading to a cyclic video.

Experiments store multiple holograms within a photorefractive crystal by assigning a unique phase distribution to the reference beam used in recording individual data pages. The novelty of this technique is in how the phase information is varied: the thickness of an elastomer mask is altered by stretching the material, introducing a shift in the optical path length traveled by each point on the reference beam. Fig. 1 is a schematic diagram of the encoding process employed in the holographic system. Two-dimensional intensity information $O(x,y)$ is recorded by a plane wave $R(x_1,y_1) = R_o\exp[i\phi_1(x_1,y_1)]\exp(ikr_1)$. The recording plane (x_3,y_3) is a distance $r_1 = [(x_3 - x_1)^2 + (y_3 - y_2)^2 + (z_3 - z_2)^2]^{1/2}$ from the mask. Phase information $\phi_1(x_1,y_1)$ is encoded on the reference beam by the elastomer, where the phase address is

$$\phi_1(x_1, y_1) = \frac{2\pi}{\lambda} n \cdot t_1(x_1, y_1) \quad (1)$$

$t_1(x_1,y_1)$ is the thickness at each point on the mask, n is the refractive index of the elastomer and λ is the recording wavelength. At the recording plane, interference between the object and reference beams leads to an intensity pattern $I(x_3,y_3)$ inside the crystal:

$$I(x_3, y_3) = |O(x_3,y_3) + R(x_3,y_3)|^2 \quad (2)$$

Via the photorefractive effect, O(x,y) is recorded as a hologram in the form of a refractive index modulation proportional to $I(x_3,y_3)$ [2]. Succeeding holograms are stored by stretching the elastomer in one dimension, introducing a different phase $\phi_2(x_2,y_2)$ given by

$$\phi_2(x_2, y_2) = \frac{2\pi}{\lambda} n \cdot t_2(x_2, y_2) \quad (3)$$

Assuming that the elastomer is incompressible and, for small displacements the stretching is uniform, the new thickness $t_2(x_2,y_2)$ is related to $t_1(x_1,y_1)$ by the conservation of volume. In the relaxed state, the elastomer mask is taken to have length L_1 and width W_1. Stretching in the present system is confined along L_1, leading to a displaced length $L_2 = (1 + \gamma)L_1$, where γ is a strain factor. The new width W_2 and a modified thickness function result from contractions of the elastomer, with the change in width negligible compared to the extension from L_1 to L_2. By further displacements from the elastomer's equilibrium state, the thickness may be easily changed to provide different phase addresses for additional data pages. For a random thickness distribution, high selectivity among recorded holograms is achieved since reconstruction with a reference beam carrying a phase code different from the original beam retrieves an amplitude O'(x,y) where

$$O'(x,y) \alpha O(x,y)\exp\{i[\phi_1 - \phi_2]\} \quad (5)$$

Intensity components of the reconstructed image tend to interfere destructively because of the random phase factor. O(x,y) is completely recovered only if the correct phase distribution is used during reconstruction. Recorded images may be reconstructed in real time by stretching and relaxing the elastomer so that the relevant phase distributions are obtained. If patterns in a specific sequence are recorded, and reconstruction is rapid enough, a holographic video may be generated. The nature of the multiplexing process with the elastomer automatically allows playback of the video in reverse and easy rewinding.

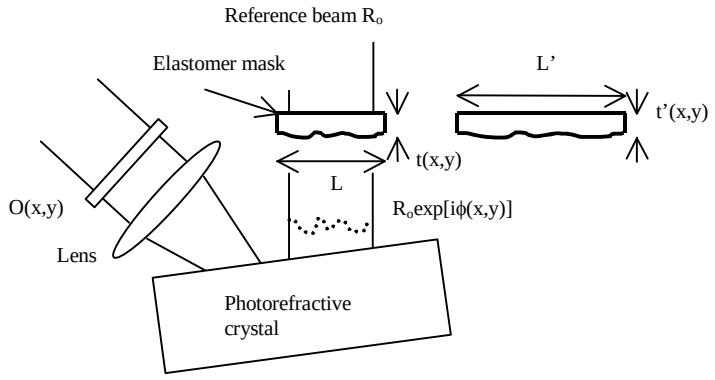

Fig. 1. Holographic multiplexing with an elastomer phase mask.

Experiments use an Ar+ laser (Spectra Physics) operating at 488 nm with an output power of 30 mW. The recording medium is a LiNbO3 crystal, doped with 0.05% Fe, having dimensions 10 x 10 x 10 mm3. A transparency in the path of the object beam contains the two-dimensional information to be recorded and a lens images the object beam into the crystal. The reference beam is encoded with phase information after passing through the elastomer mask. Recording is not done at the Fourier plane.

Masks are prepared from Sylgard 184 silicone elastomer. Random phase information is imprinted on the elastomer by first applying a thin layer of quick-drying adhesive nonuniformly on the bottom of a glass dish. Sylgard is then poured into the container where the elastomer flows into all available gaps on the hardened adhesive. After a sufficient amount of curing time, the elastomer solidifies, with one surface taking exactly the

same three-dimensional profile as the layer of adhesive, and is peeled off from the glass surface. The nonuniform application of adhesive results in a random thickness distribution for the solid elastomer. A special holder is constructed for mounting the elastic phase mask. Both ends of the mask are fastened securely by clamps and displacements in one direction are obtained by hand-turning a screw mechanism.

Through the linear electro-optic effect, interference between the input object and the phase-coded reference beam modulates the refractive index of the crystal, storing the information as an erasable hologram. Upon blocking the object beam, diffraction of the reference beam retrieves the stored information. A CCD

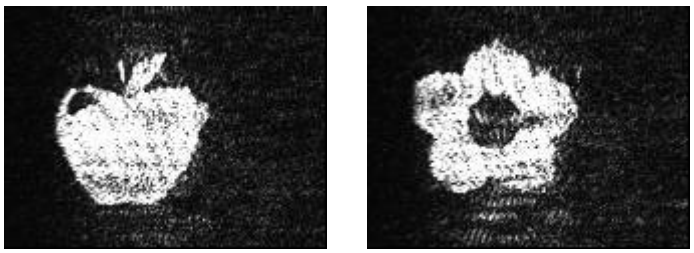

camera captures the recovered image. Fig. 2 is a collection of images reconstructed from the experiments.

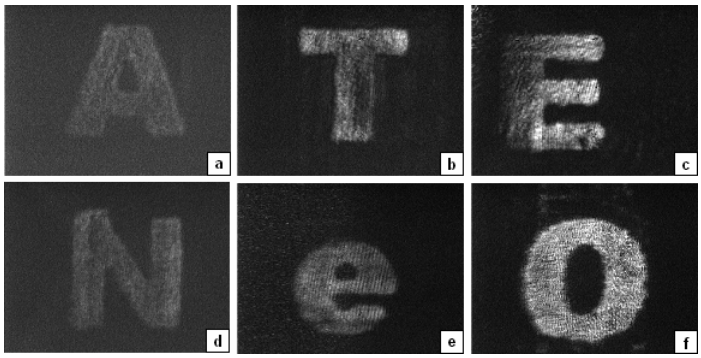

Figure 2. Reconstructed images from holograms recorded with an elastomer phase mask.

Good reconstruction is obtained for all images, even with the random phase distribution of the reference beam, and no crosstalk is observed. In the experiments, the minimum strain interval required to create an appropriate phase disparity for recording additional holograms varies due to the random thickness distribution of the mask. Sensitivity of the phase distribution imprinted on the elastomer mask to stretching is determined by the mold used in fabricating the Sylgard sample. In a single elastomer sample, different regions encode the reference beam with phase information at varying levels of displacement sensitivity. Using displacements of 0.21 mm, approximately 45 holograms may be stored with a mere 10% strain on the elastomer. Improving the random thickness distribution in the elastomer mold, such that smaller stretch intervals are required for phase mismatch, would increase the theoretical multiplexing capacity.

Holographic animation sequences are generated by multiplexing successive frames of a moving object and reconstructing the holograms rapidly in real time. Fig. 3 consists of frames from a holographic video obtained using the experimental set-up. The video is of a circular fan moving clockwise then counter-clockwise. Alternately stretching and relaxing the phase mask allows for cyclic playback. Due to manual displacement of the elastomer during animation, the frame rate ranges from 8 to 25 fps, based on the transition time between successive images. If the total time for an entire sequence is considered, the average frame rate is approximately 6 fps, the maximum possible with the present holder and mode of stretching the elastomer. Although currently slower than the standard 25 fps on average, the animation results clearly show the efficacy of the holographic technique.

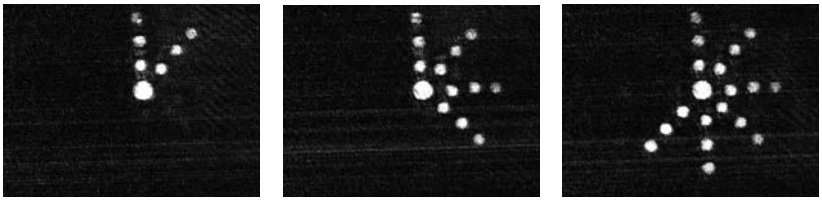

Figure 3. Successive frames from a holographic video sequence.

III. STRETCHABLE Au-COATED DIFFRACTION GRATINGS

Regarding diffractive elements, stretchable silicone gratings show promise as dynamic beam scanners but are usually limited to transmission applications because of the low reflectivity of the material. Reflection gratings, however, are more commonly used and lead to higher efficiencies, compact systems and fewer constraints regarding wavelength and diffraction angle [3]. The same transparency that makes transmission configurations convenient then becomes a liability as silicone gratings possess inherently low reflectivity. This section describes how the efficiency of a stretchable diffraction grating in reflection mode is improved by coating the sample with a thin layer of Au [4]. Experimental results indicate that the performance of the grating as a beam scanner is affected by the surface structures resulting from the interplay between the stiff metal skin and flexible silicone substrate. Elastomeric gratings act as dynamic beam scanners with variable diffraction angles by the modification of groove spacing through mechanical stretching. The enhancement in reflectivity afforded by the Au coating tends to decline as buckling structures evolve on the metal surface in response to the change in length of the elastomer.

A stretchable diffraction grating is fabricated by imprinting the ruled surface of a plane reflection grating onto an elastomer layer. An amount of the prepared silicone is poured into a glass dish to produce a layer approximately 1 mm thick. Once the elastomer sample settles, the grating is pressed down on the surface slowly, with care to avoid the formation of bubbles at the metal-silicone interface. Total pressing time is equivalent to the curing period of seven days. Room temperature throughout this time interval is maintained at 25 oC. The master grating is a high-quality aluminum-coated replica from Edmund Scientific, with the original made on an interferometrically-controlled ruling engine. Grating area is 2.54 cm x 1.27 cm, with a triangular groove profile at 1200 lines/mm (groove spacing d = 0.833 μm) and a blaze wavelength of 400 nm. After sufficient curing of the elastomer, the master is carefully peeled off, leaving a perfect copy of the grating surface imprinted on the silicone. For convenient mounting of the sample, we cut out a section of the elastomer measuring 6.5 cm x 3.3 cm, placing the grating at the center. Reflectivity of the grating is then improved by the addition of a thin Au layer. Coating of the sample is done via thermal evaporation using resistive heating at a base pressure of 4 x10-5 mbar. A 7 nm layer of chromium is first deposited to improve adhesion between Au and silicone. Au thickness is set to 100 nm, achieved at a deposition rate of 0.1 nm/sec. Fig. 4 shows the final coated grating produced from the fabrication process. The area of the elastomer with the Au layer is translucent. White light dispersion is readily observable on the grating section, although the effect may also be seen, to a lesser extent, with an uncoated version. No appreciable change is perceived in the coated silicone's flexibility. Viewing of a typical region of the coated grating at 100X magnification verifies that the replicated grating grooves are well-defined at a uniform d = 0.833 μm, consistent with the metal master. Metal globules, artifacts of the deposition process, are evident on the film surface. Wrinkles are already present, even at zero applied strain, and these same surface faults will serve as imperfection sites for extensive buckling effects as the elastomer grating is elongated.

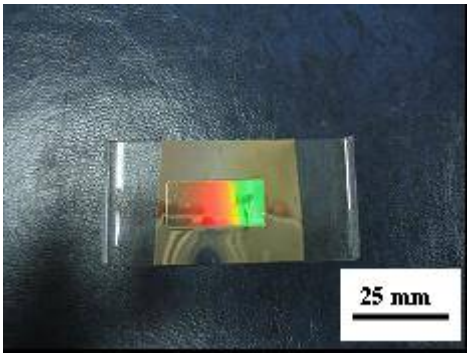

Figure 4. A diffraction grating fabricated from silicone.
The surface has been coated with a thin Au layer.

The influence of a homogeneous compliant substrate on a thin metal film is described by the stress σ. In our beam scanning experiments, the coated grating is stretched in one direction, perpendicular to the grooves. The nonuniform levels of stress along the two axes (σ_x and σ_y) determine the alignment of buckling features formed on the Au layer. Larger buckling effects emerge at farther distances from the stationary side of the distending material. At the point where the elastomer is fixed (x = 0), the stress in the x-direction is zero. In the y-direction, σ_y is given by:

$$\sigma_y = -\sigma_o[1 - \nu\exp(-x/x_o)], \qquad (6)$$

where x is the distance from the static end and x_o is a transition length dependent on film thickness and material properties. Cooling of the sample after the deposition process produces a natural compressive stress σ_o and ν is the effective Poisson ratio. Stress parallel to the grating grooves varies as a function of position along the x-axis, with larger values manifesting at sites closer to the moving edge. Diffraction experiments investigate how this evolution of buckling features with increasing strain affects the efficiency of coated stretchable gratings.

Fig. 5 is a schematic diagram of the system used for diffraction experiments. The light source is a HeNe laser (Uniphase) with λ = 632.8 nm operating at an output power of 1 mW. One of the clamps holding the sample is attached to a screw mechanism that, when manually turned, stretches the elastomer in one direction. For simplicity, diffraction is observed with a P-polarized beam (diameter = 0.48 mm) at normal incidence on a point at the center of the grating, 36 mm from the stationary edge of the sample. Scanning capability of the stretchable grating in reflection mode is verified by measuring the angular deflection of the 1st-order diffraction as the elastomer is subjected to strain levels ranging from 0 to 7.6%. The behavior of diffraction angle vs. strain $s = \Delta L/L_o$, where L_o = 25.4 mm, is summarized in Fig. 6. For this strain interval, a $\Delta\theta = 2.34^o$ is achieved by a 2 mm elongation of the grating. The functioning of the sample is stable over multiple extensions and relaxations. Scanning range of the diffracted beam for a set amount of strain is dependent on which area of the grating the laser is incident on: $\Delta\theta$ is variable with respect to groove location.

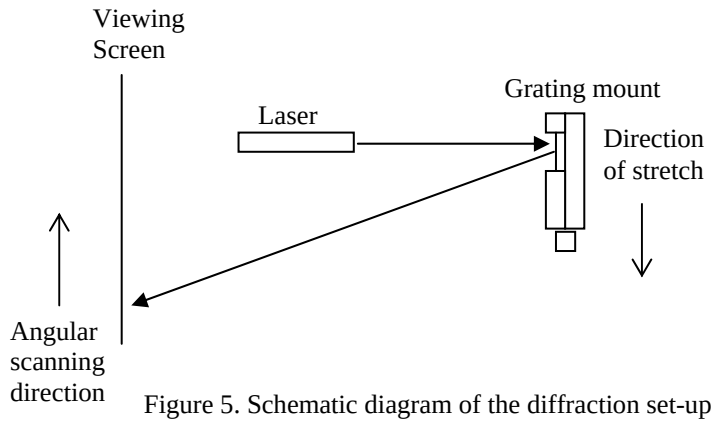

Figure 5. Schematic diagram of the diffraction set-up with the beam at normal incidence.

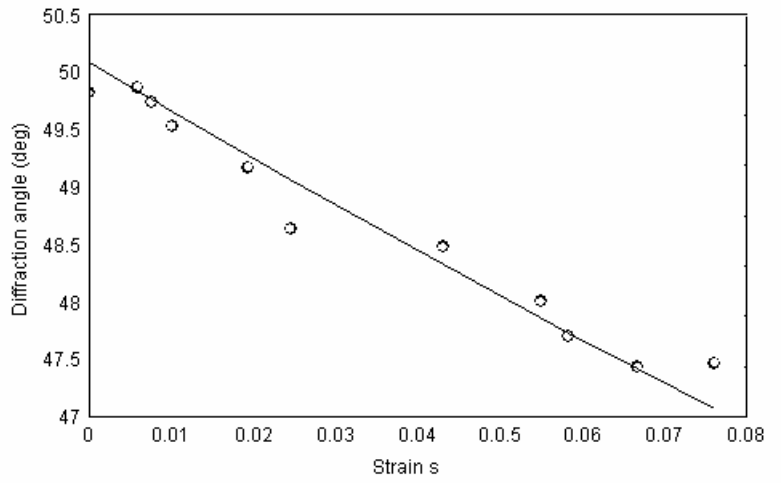

Figure 6. Angular scanning in stretching mode of the 1st-order diffraction as a function of strain.

Measurements indicate that the efficiency of the stretchable grating drops as reflectivity of the Au film degrades because of spontaneous buckling structures. Changes in the grating structure imprinted on the surface are to be expected as the elastomer is extended. Stretching the sample will affect the height of the grooves as the elastomer deforms to conserve volume. However, at the strain levels involved in characterizing the grating, the change in groove height is taken to be negligible and reflectivity of the Au coating becomes the dominant factor. To emphasize the improvement in efficiency when an Au layer is added, we obtain the enhancement ratio η/η_o where η and η_o are the grating efficiencies of the coated and uncoated samples, respectively. The low reflectivity

of the material, coupled with the arbitrary angle of incidence, yields an uncoated efficiency η_o = 0.11%. Enhancement as a function of strain is plotted in Fig. 7. The separate data sets, designated AR1 and AR2, correspond to distances of 48 mm and 36 mm from the static edge, respectively. Improvement in efficiency is consistently higher when the beam is incident on AR2, with an enhancement factor of ~50, as compared to AR1's maximum η/η_o of ~40, at zero strain. Differences in the initial enhancement are characteristic of a sample that has undergone numerous scanning cycles. Permanent defects in the Au layer, brought about by more intense compressive stress in the moving region and present even when the sample is unstretched, produce the smaller η/η_o values obtained from AR1. As the strain levels rise, efficiency drops as buckling structures develop on the metal surface. AR2, located in a section of the elastomer experiencing weaker compressive stress, is less susceptible to buckling effects on the Au film. Even when compared to diffraction from an uncoated sample in a transmission configuration, the Au-coated grating in reflection mode has η/η_o = ~20.

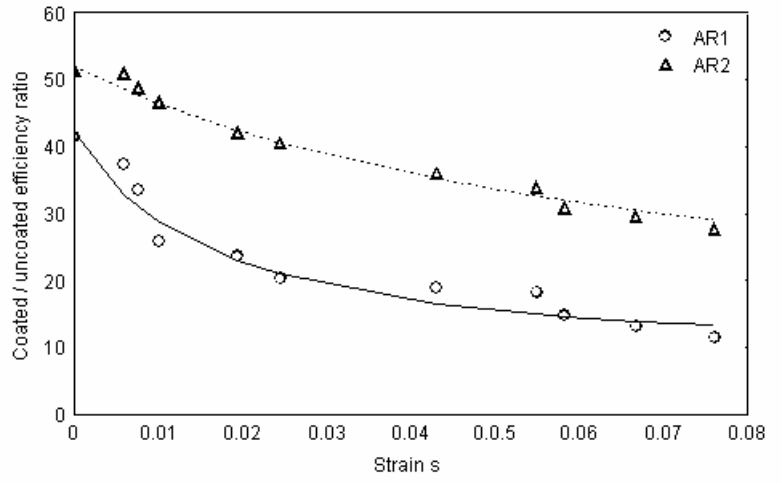

Figure 7. Improvement in diffraction efficiency from the Au coating decreases with strain.

IV. FLUORESCENT DYE-DOPED ELASTOMERS

One particularly promising aspect of elastomeric optics deals with doping a polymer host with a fluorescent dye. The initial experiments reported here require the silicone to be prepared in the form of thin rectangular strips. A bulk sample is made from Sylgard 184. The silicone is mixed with a 2 ml solution of chlorophyll in acetone. Final chlorophyll concentration in the silicone is 1.5 x 10^{-3} M. Uniform distribution of the dye is achieved after continuous stirring of the mixture for several minutes. The dye-doped silicone is then poured into a mold, where the sample is left to cure for five days at 25^o C. Over the curing period, the acetone evaporates completely. The silicone is peeled off the mold and cut into appropriate sections. Fig. 8 is a photograph of a fabricated chlorophyll-doped elastomer strip under white light. The silicone remains transparent, tinged only by the signature color of the dye. Flexibility of the sample is not affected by the doping procedure. Chlorophyll is evenly dispersed throughout the volume of the strip and is fully encased within the elastomer. No smearing is observed when the dye-doped strip comes into contact with another surface.

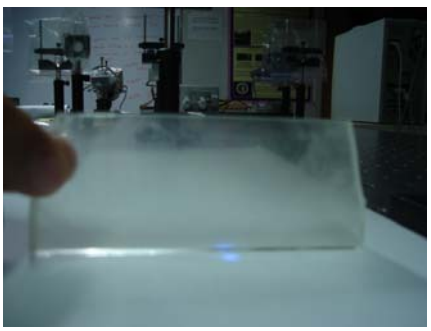

Figure 8. Elastomer strip doped with chlorophyll under normal illumination.

Under UV illumination, the sample fluoresces as observed in Fig. 9. Photoexcitation is provided by a Q-switched diode-pumped Nd:YVO_4 laser (CrystaLaser) with λ = 355 nm, 20 kHz repetition rate and an output power of 25 mW. The photograph is taken in darkness to enhance visibility of the fluorescence. Characteristic

emission in the red for chlorophyll is prominent along the laser beam. Chlorophyll in silicone displays a characteristic broadband spectrum resulting from a large number of vibrational and rotational energy levels associated with the organic molecules [5] with peak wavelength at 660 nm (Fig. 10). Full-width-at-half-maximum (FWHM) is 20 nm. As with similar elastomer-based optical elements, potential sensors using dye-doped silicone have the advantages of economy, versatility in sample design and undemanding fabrication methods.

Figure 9. Fluorescence from a chlorophyll-doped elastomer with UV excitation.

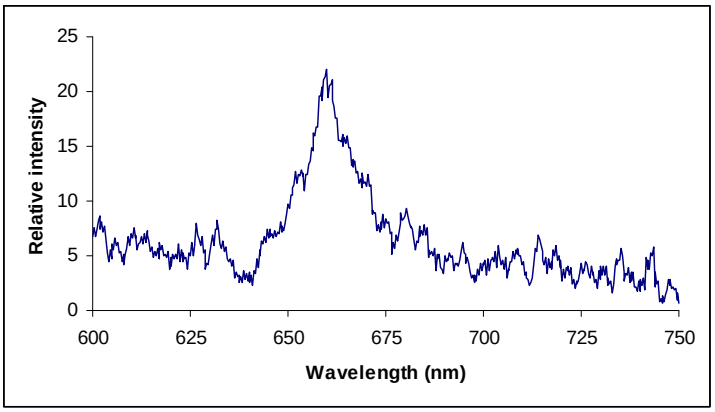

Figure 10. Fluorescence spectrum for chlorophyll immobilized in silicone excited at 355 nm.

IV. SILICONE REPLICATED OPTICS FOR INTRODUCTORY SCIENCE EXPERIMENTS

Basic experiments for the grade school level that make use of silicone lens and grating replicas are being designed and tested in pilot classrooms. As part of the requirements for a graduate course, a public school teacher volunteered to use elastomeric lenses and diffraction gratings as demonstration tools for her sixth-grade science class. Her motivation was to allow the students to experience optics through a hands-on activity. The usual scenario in Philippine public schools is that laboratory resources are very limited and students rarely have the opportunity to actually handle equipment. Due to the low cost of the replicated silicone optics, materials can be made readily available and care in handling them is less of a concern.

In Fig. 11 is a lens similar to the one used by the sixth-graders. Also included is part of the activity sheet distributed in class. On the sheet is a simple procedure to follow and guide questions for the experiment. The student who accomplished this sheet made the observation that his silicone lens "produces a larger size and is better to handle".

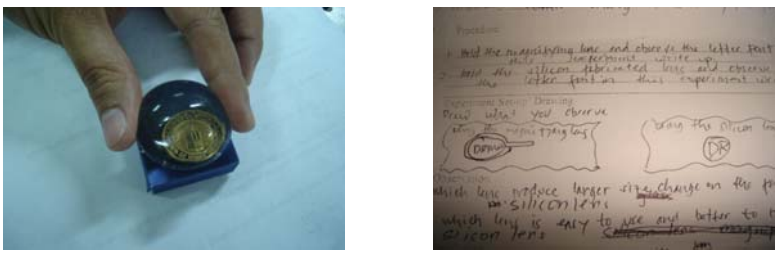

Figure 11. Left: An elastomer lens replica and right: a grade school optics activity sheet.

The silicone diffraction grating and its corresponding activity sheet are shown in Fig. 12. White light dispersion may be seen on the grating surface and students are quick to notice this. All the students were able to illustrate a rainbow spectrum on their papers. For her conclusion regarding the activity, one student stated that gratings are used "to change white light into many colors". She also noted that "white light is not totally white but has many colors". The teacher who facilitated the experiments found the activities to be very rewarding and hopes that this experience will further develop her students' love for science.

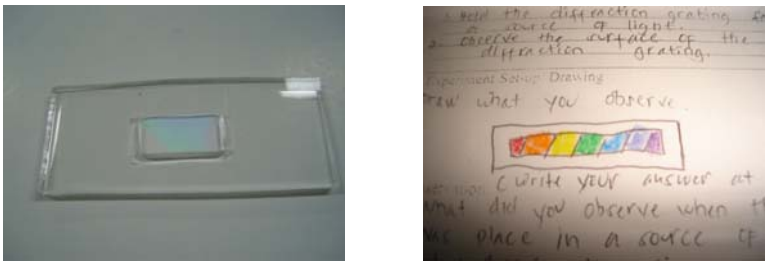

Figure 12. Left: a silicone diffraction grating displaying white light dispersion and right: observations from a sixth-grade student.

V. FUTURE PROSPECTS

Work on volume holography and deformable diffraction gratings continues at the Ateneo Photonics Laboratory. Much attention is currently being given to the development of new sensors based on fluorescence from dye-doped elastomers. Novel protocols in immobilizing different dyes in silicone are being investigated. Financial support for our research is provided by the Philippine Council for Advanced Science and Technology Research and Development.

References:

[1] R. A. Guerrero, "Volume holographic storage and animation based on addressing with an elastomer phase mask", Optics Communications V245 N1-6, 75-83 (2005).

[2] P. Yeh, Introduction to Photrefractive Nonlinear Optics, Wiley, New York, 1993.

[3] E. Loewen, E. Popov, Diffraction Gratings and Applications, Marcel Dekker, New York, 1997.

[4] R.A. Guerrero, J.T. Barretto, J.L.V. Uy, I.B. Culaba and B.O. Chan, "Effects of spontaneous surface buckling on the diffraction performance of an Au-coated elastomeric grating", Optics Communications V270, 1-7 (2007).

[5] D. Rendell, Fluorescence and Phosphorescence Spectroscopy, Wiley, Chichester, 1987.